

日本原子力研究開発機構機関リポジトリ
Japan Atomic Energy Agency Institutional Repository

Title	Wet granulation of mixed oxide powders de-nitrated by the microwave heating
Author(s)	Yoshiyuki Kato
Citation	Journal of Nuclear Science and Technology,49(10):p.999-1009
Text Version	Author
URL	http://jolissrch-inter.tokai-sc.jaea.go.jp/search/servlet/search?5034151
DOI	http://dx.doi.org/10.1080/00223131.2012.723176
Right	This is an Author's Accepted Manuscript of an article published in [include the complete citation information for the final version of the article as published in] the Journal of Nuclear Science and Technology, 2012 ©Taylor & Francis, available online at: http://www.tandfonline.com/10.1080/00223131.2012.723176

1. Introduction

In the fabrication process of oxide fuels for light water reactors (LWRs) and fast breeder reactors (FBRs), the raw powder is usually granulated before pressing. Organic powders such as polyvinyl alcohol and zinc stearates are commonly mixed in as a binder or a lubricant. This mixing process causes dispersion of the raw powder in the glove box, which is the main source of radioactive exposure to workers. The organic powders are removed in a preliminary heating apparatus at around 800°C, before sintering [1]. However, the residue and its decomposed products contaminate the sintering gas atmosphere and deposit on the exit of sintering furnace and the ventilation duct, which results in frequent clean-up operation and reduces the life-time of the furnace.

If water is used instead of the organic powder as a binder, most of the water in the raw powder could easily be removed by drying it around 100°C before the pressing process. In addition, the current granulation process could be simplified because granulation using water could be done simultaneously with production of raw powder. Which is a significant merit especially in uranium-plutonium mixed oxide (MOX) fuel fabrication [2].

A new granulation method for MOX raw powder was examined in a small-scale hot apparatus by using water as a binder. The raw powders were prepared by the microwave heating (MH) de-nitration method that had been developed and demonstrated for FBR fuel fabrication in Japan. BET specific surface areas and particle size distributions were measured and fine structures were observed by scanning electron microscopy (SEM) before and after the granulations. Bulk density, tap density, compressibility, repose angle, spatula angle, and aggregate ratio (uniformity) were measured then flow-ability was determined from these results based on the ASTM method [3] [4] before and after the granulation. Finally, the granulation performance was discussed.

This study was performed as a part of the study on simplified pelletizing fuel fabrication system [5] adopted by the Fast Reactor Cycle Technology Development Project (FaCT Project) [6] promoted by the Japan Atomic Energy Agency (JAEA).

2. Experimental procedures

2.1. Samples

In this study, 14 samples of MOX raw powder and three samples of UO₂ raw powder were prepared and examined at the Plutonium Conversion Development Facility. Samples were prepared from plutonium nitrate (Pu(NO₃)₄) solution and uranyl nitrate (UO₂(NO₃)₂) solution taken from the solutions separated and purified from the spent nuclear fuel at the Tokai Reprocessing Plant of JAEA. For the MOX samples, these solutions were mixed to compose the ratio of 20 wt% Pu-80 wt% U, and then the mixture or the uranyl nitrate solution was de-nitrated in a shallow dish for around 50 minutes in a microwave heating apparatus (2.45 GHz, 5 kW) according to our standard procedure.

Table 1 summarizes the specifications of examination apparatuses used in this study. Figure 1 illustrates the structure of the microwave heating apparatus that supplies microwave energy from outside the glove box (GB) to the oven set up inside the GB through the waveguides. The capacity of the oven was about 250 liters, however the volume of mixed solution supplied to the shallow de-nitration dish was two liters/batch. The whole view of microwave oven installed inside the GB is shown in Figure 2. Details of the MH method have been presented in the previous papers [7][8][9]. Obtained material by the de-nitration was calcined at 750 °C for two hours in the air, and then the oxide (U₃O₈ - PuO₂ or U₃O₈) was reduced to mixed dioxide or uranium dioxide at the same temperature under the N₂-H₂ mixture gas. The electric furnace with a rotary pod inside the furnace used for calcination and reduction is shown in Figure 3. Around 600 gram of dioxide was obtained from each de-nitration batch and used for a sample.

2.2. Characterization

Table 2 summarizes the specifications of analytical apparatuses used in this study. BET specific surface area was measured with a gas flow type measurement instrument (Shimadzu Flow Sorb II 2300) for both the raw powder and the granules. Particle size distribution of the

raw powder was measured in water with a laser type analyzer (Horiba LA-920). When the raw powder is granulated, the particle size become extremely large compared to that of raw powder and the distribution cannot be measured by the same method due to its size. Therefore, the particle size distribution of granules was measured by sieving the granules through nine meshes of successively smaller sizes (1,000 μm , 850 μm , 710 μm , 500 μm , 355 μm , 250 μm , 150 μm , 75 μm , and 45 μm).

In order to determine the flow-ability of the raw powder and the granules, bulk density, tap density, compressibility, repose angle, spatula angle and aggregate ratio (uniformity) were measured with a type PT-S powder tester (Hosokawa Micron). After the measurements, a point was given for each measurement result according to the point score table, and then an index corresponding to flow-ability was derived. Details of the measurement and the derivation are described in Carr's paper [3] and ASTM D6393-08 [4].

Furthermore, particle distribution at low magnification and fine structure at high magnification of the raw powder and the granules were observed with a scanning electric microscope (Hitachi S-4300).

2.3. Granulation

Figure 4 illustrates the agitating granulator (LFS-5 type high-speed mixer made by the Fukae pawtec company) used in this study. The granulator has three agitation blades rotating on the bottom for compressing, kneading and granulation and a chopper blade on the wall to fracture huge granules. The inner diameter of the granulator vessel was 230 mm and its height was 140 mm. The diametrical clearance between the outer surface of the blade and the inner surface of the granulator vessel was less than 1.0 mm. About 600 gram of powder was put into the granulator and granulated at 650 rotations per minute (rpm) as the blade rotation speed.

Water was added by spraying a predetermined amount from the upper side of the granulator. After granulation, excess water was removed by heating the granules at 80 °C in the air for

two hours. Then, the dried granules were sieved into 1.0 mm mesh to exclude remaining huge granules, because such granules bring lack of uniformity in density and they cannot be applied to the pressing process.

3. Results

Table 3 summarizes BET specific surface areas and average particle sizes of the UO₂ raw powder and the MOX raw powder. The range of BET specific surface area was 1.5 to 2.0 m²/g for UO₂ and 2.4 to 3.8 m²/g for MOX. The range of average diameter was 1.0 to 1.5 μm for UO₂ and 1.2 to 1.8 μm for MOX. Although the UO₂ raw powders and the MOX raw powders are prepared by the same experimental condition, there is a trend in BET specific surface area that the results for MOX are a little larger than those for UO₂. In addition, variations are seen both in UO₂ and in MOX. The reason of variation is considered to be a small difference of batch treatment for each sample. For average diameter, the difference between UO₂ and MOX is not significant. The BET specific surface area for the MOX raw powder is good for sintering.

Table 4 summarizes other characteristics of the raw powders, bulk density, tap density, compressibility ratio, repose angle, spatula angle, and aggregation ratio, measured with the powder tester, together with index of flow-ability. The index of flow-ability was 26 to 31 for the UO₂ raw powder and 18.5 to 26 for the MOX raw powder, which were categorized as "Low" determined by the manufacturer of the powder tester. In fact, they are inadequate to achieve smooth flow neither in a handling apparatus nor in a pressing apparatus.

Figure 5 shows SEM photos at two magnifications of the UO₂ raw powder and the MOX raw powder. In Figs. 5(a) and (c) taken at a low magnification, it is observed that both powders are well dispersed. In Figs. 5(b) and (d), at high magnification, it is observed that a number of fine particles (0.1 μm or less in diameter) agglomerate to form a larger particle (2nd particle). The appearance of UO₂ 2nd particle is different from that of MOX 2nd particle, which may correspond to the difference in BET surface area in Table 3.

The average diameter of the agglomerated particle (2nd particle) is 1 to 2 μm by laser as shown in Figure 7. In particle size distribution measurement by laser, the raw powder is scattered in water then measured. Therefore, the result is different from that measured by SEM observation in a vacuum, because the 2nd particle loses cohesion and collapses in water due to its weak cohesive force and then agglomerates again.

Table 5 summarizes the results of granulation, BET specific surface area and average particle size and product yield in relation to the water addition ratio. The ratio is the weight of added water divided by the total weight. The product yield is the weight of granules excluding huge granules ($> 1.0 \text{ mm}$) divided by the total weight of granules.

As a result, we were successfully able to obtain granules over 100 μm in diameter both for UO_2 and for MOX. Especially, it was important that the BET specific surface area of MOX granules was almost the same as that of raw powder, which suggested good sintering performance of the granules. From the viewpoint of producing efficiency, it was important that the product yield of MOX granules was $> 90 \%$ within the range of water addition ratio from 12.5 to 13.5 wt% where MOX granules of 120 to 140 μm in diameter were successfully obtained. In the samples MOX-1 to MOX-4 of this table, average particle size and product yield were not written because no granules were obtained. In addition, the product yield decreased significantly in response to the increase of water addition ratio.

Table 6 summarizes another characteristic of the granules in relation to the water addition ratio, bulk density, taps density, compressibility ratio, repose angle, spatula angle, and aggregation ratio, measured with the tester, together with index of flow-ability. From the viewpoint of performance, it was important that the index of flow-ability of MOX granules was > 70 within the narrow range of high product yield mentioned above. This value was categorized as "High" determined by the manufacturer of the powder tester. Thus, it is possible to combine high flow-ability and high product yield within the range of water addition ratio from 12.5 to 13.5 wt%. However, the index of flow-ability of MOX granules did not change from that of MOX raw powder if water addition ratio was $< 11 \text{ wt}\%$. It looks

like that a boundary lies between 11 wt% and 12.5 wt%. Such boundary looks like exists in bulk density, compressibility, repose angle and aggregate ratio.

Figure 6 shows changes in the flow-ability and the product yield of MOX granules in response to water addition ratio. It is estimated that the flow-ability started to rise sharply from < 30 to > 70 when the water addition ratio was 8 to 9 wt%, which is the 2nd boundary. Between two boundaries, the MOX raw powder seems to be partially granulated. On the other hand, powder/granules with flow-ability > 60 are considered, in general, to be adequate to achieve smooth flow. This value corresponds to the water addition ratio around 12.5 wt% by interpolation. As a result, the MOX granules obtained in the water addition ratio > 12.5 wt% could be used and 13.5 wt% is sufficient, where high product yield > 90 % and high flow-ability > 70 are also obtained. If the ratio is > 14 wt% (the 3rd boundary), the product yield rapidly decreases because the ratio of huge granules (> 1.0 mm) increases, which is the result of sieving by a mesh.

Figures 7 and 8 show particle size distributions before and after the granulation measured by laser or by sieving. The particle size before granulation increase nearly 100 times by granulation. There is a trend that the UO₂ granules are larger than the MOX granules though the UO₂ raw powder particles are smaller than the MOX raw powder particles. For the MOX, the fraction of small granules/particles of less than 45 μm reaches to 5 % in Figure 8. These particles may easily adhere to the wall of granulator, and then bring a little loss of production yield. Such small granules/particles were not excluded in this study because there had been no empirical criteria for the smallest diameter. Moreover, the ratio (5 %) becomes smaller if production scale becomes larger. However, it may be reasonable that the criteria will be set up to be 45 μm because mechanical sieving could be applied.

Figure 9 shows SEM photos at two magnifications of the UO₂ granules and the MOX granules. When the low magnification Figs. 9(a) and (c) are compared to Figs. 5(a) and (c), it is apparent that the raw powder particles agglomerate and is well granulated. In addition, the high magnification Figs. 9 (b) and (d) show a small difference in microstructure between UO₂

and MOX, which may corresponds to the difference in BET surface area in Table 5.

4. Summary of experimental results

- 1) We were successfully able to obtain the granules over 100 μm in diameter both for UO_2 and for MOX. Especially, it was important that the BET specific surface area of MOX granules was almost the same as that of raw powder, which suggested good sintering performance of the granules.
- 2) From the viewpoint of producing efficiency, it was important that the product yield of MOX granules was $> 90\%$ within the range of water addition ratio from 12.5 to 13.5 wt% where MOX granules of 120 to 140 μm in diameter were successfully obtained.
- 3) From the viewpoint of performance, it was important that the index of flow-ability of MOX granules was > 70 within the narrow range of high product yield mentioned above. This value was categorized as "High", based on the point scores described in Carr' paper [3] and ASTM D 6393-4 [4].
- 4) It is possible to combine high flow-ability and high product yield within the range of water addition ratio from 12.5 to 13.5 wt%.
- 5) As a result, MOX granules obtained in the water addition ratio > 12.5 wt% could be used and 13.5 wt% is sufficient, where high product yield $> 90\%$ and high flow-ability > 70 are also obtained. The product yield decreases if water addition ratio > 14 wt%.

5. Discussion

We would like to discuss the stepwise change in flow-ability in response to water addition ratio (wt %) shown in the Figure 6. The flow-ability does not change if water addition ratio is lower than 8 to 9 wt%. In fact, no granule was observed within the range.

It is commonly accepted that the binding force between particles at granulation by adding water comes from the liquid bridges between particles. Within this flat response range, it is estimated that the liquid bridges does not exist or grow insufficiently though some water is

added. Such phenomenon is observed by Fuji [10] in porous silica particles. Water added to the porous particle initially invades into the pores inside the particle as capillary flow, which brings difficulty in formation of liquid bridges between particles. This mechanism looks like probable because we have observed by SEM both in Figure 5 and reference [1] that the raw powder particle (average diameter is 1 to 2 μm by laser) before granulation has a lot of internal gaps. These gaps formed by agglomeration of more fine particles (0.1 μm or less in diameter by SEM). The raw powder particle is now called "2nd particle".

To confirm this mechanism and to estimate the degree of porousness of the 2nd particle, we measured density of a granule (around 0.5 mm in diameter as shown in Figure 11) by weighing it on a glass dish and by reading diameter under a microscope one by one. Average of the obtained density was, as a matter of course, lower than the theoretical density of uranium/plutonium dioxide (11 g/ml). Then, we estimated average density of the 2nd particle supposing the closest packing. The result was 5.5 g/ml (just half of the theoretical density), so the volume ratio of pores in the 2nd particle was estimated to be 0.50. If pores are filled by water, the ratio of water weight divided by the total weight is 1/12 or 8.3 % which corresponds to the upper limit of the flat response range. This is rough evaluation where water weight in pores and liquid bridges are neglected due to the large difference of true density between water and dioxide; however the result of precise evaluation is not so different. Therefore, we could confirm the mechanism of the flat response range.

Then, let us discuss the sudden increase and saturation of flow-ability next to the flat response range. When water addition ratio is 8 to 9 wt%, flow-ability is < 30 and no granule was obtained. When water addition ratio is 12.5 to 13.5 wt%, flow-ability reaches to > 70 and product yield reaches to > 90 %. If the ratio is larger than 14 wt%, the product yield decreases whereas flow-ability does not change. Thus, the best condition is very narrow.

However, such phenomenon is normal in granulation theory where a small stable liquid bridge connecting two particles and not overlapped between three or more particles is the best. This is called "Pendular state" [11]. Let us assume a bridge between two equi-sized contacting

spheres shown in the Figure 10. The ratio of bridge volume divided by volume of two spheres is around 5.3 %, if cross-section curve of the bridge is approximated to be an arc, contact angle θ is zero because the surface is wetted due to the filled water in pores, and the center radius of bridge r_2 is the same as the other center radius r_1 . The last condition $r_2 = r_1$ is the requirement from dynamics for the stable shape of liquid bridge between unfixed two equi-sized spheres when water is given sufficiently, because its surface has a symmetry of rotation and the cross-section curve is catenary. The volume ratio 5.3% is converted to the water addition ratio to be 1.0 wt% supposing the sphere density as 5.5 g/ml. However, the converted ratio is smaller than the difference of water addition ratio between 8 to 9 wt% and 12.5 to 13.5 wt%, which is 4.5 ± 1 wt%.

To solve this problem, we considered multi-link model where a particle has 1/2 (for two particles) -6 (for closest packing) liquid bridges those are not overlapped. Increase of water addition ratio per a link is twice (2.0 %) of the converted volume ratio. The water addition ratio of 4.5 ± 1 wt% corresponds to 2.0 to 2.5 links (liquid bridges) per a particle. We think it normal in the Pendular state. It is, however, difficult to discuss the relationship between the water addition ratio and the average particle size of the granule.

Concerning the liquid bridge, the following equation is usually quoted as "Young-Laplace equation" but it is modified from the original. ΔP_L denotes the negative pressure due to the surface curvature of liquid bridge:

$$\Delta P_L = \sigma \left(\frac{1}{r_1'} - \frac{1}{r_2'} \right) \dots\dots\dots (1)$$

where r_1' and r_2' are arbitrary curvature radius of the bridge surface (see Figure 10) and σ is the surface tension. This equation is very general, however in the case of $r_1' \approx r_2'$, the effect of negative pressure is very small. On the other hand, the binding force F_L due to the liquid bridge is composed of two components known as Gorge method [12]

$$F_L = \pi (r_2')^2 \Delta P_L + 2\pi (r_2') \sigma$$

where r_2' is the radius r_2' at the center of the bridge. The 1st term is the contribution of

negative pressure (this term is negligible if $r_1' \approx r_2'$) and the 2nd term is the contribution of the surface tension. F_L is calculated from the 2nd term to be 2.3×10^{-7} N, because $r_2 = 0.68 \times r_0$, $r_0 = 0.75 \mu\text{m}$ (half of the observed average particle diameter) and $\sigma = 0.072$ N/m. On the other hand, force of gravity acting the particle is only 1.0×10^{-13} N, supposing the sphere density as 5.5 g/ml. It was confirmed that the binding force is extremely larger than the force of gravity. We estimate that granulation proceeds by the binding force where 2nd particles are packed very closely in a granule.

Therefore, we were able to confirm the reason of sudden increase and saturation of flow-ability, based on the consideration of small stable liquid bridges connecting two or more particles in Pendular state, when water is given sufficiently. Excess water does not contribute to the binding force, which results in saturation of flow-ability and yield of huge granules.

5. Conclusion

In this study, 14 samples of MOX raw powder and three samples of UO_2 raw powder were prepared by calcination and reduction of de-nitrated material obtained by MH method. Performances in wet granulation were examined using agitating granulator with three blades and a chopper. Characteristics and physical properties of the raw powder and the granules were measured together with observations by SEM before/after granulation. BET specific surface area, particle size distribution, bulk density, taps density, compressibility ratio, repose angle, spatula angle, and aggregation ratio were measured, and then index of flow-ability were derived.

When the raw powders were granulated by adding water in an amount around 13 % of their weight, the powder flow-abilities exceeded 70 and they were well granulated. The diameters of obtained granules were 120 to 140 μm whereas the diameters of raw powder were several μm . The product yield exceeded 90 %. Specific surface area that corresponds to sintering performance was almost the same as that of raw powder. If the water addition ratio was < 9 wt%, granulation did not start because of the difficulty of liquid bridge formation. If the ratio

was 11 wt%, granulation starts but flow-ability was insufficient. If the ratio was > 14 wt%, flow-ability saturated and product yield decreased. The appropriate narrow range of water addition ratio was 12.5 to 13.5 wt% combined with high flow-ability > 70 and high product yield > 90 %.

The boundary value 9 % added water by weight for whether the granulation starts or not, corresponded to the complete filling of water in capillaries (or voids) inside the raw powder particle. The boundary value 14 % added water by weight for whether the granulation saturates or not, corresponded to the filling of water in liquid bridges outside the raw powder particle. The narrow range of water addition ratio was successfully understood based on the standard theory of granulation supposing "Pendular state" where a small stable liquid bridge connecting two particles and not overlapped between three or more particles, when water is given sufficiently.

The binding force was calculated by "Gorge method" using measured average diameter of the raw powder and the small stable liquid bridge. The result was extremely larger than the gravity force of two raw powder particles, thus it was understood that granulation proceeds by the binding force where raw powder particles are packed very closely in a granule.

Acknowledgements

The author wish to express special thanks to Dr. H. Furuya, Emeritus Professor of Kyushu University and Dr. T. Hosoma of JAEA, for valuable discussions and suggestions. The author is also grateful to all the people who supported our experiment

References

- [1] K. Asakura, Y. Kato, H. Furuya, Characteristics and sinterability of MOX powder prepared by the microwave heating denitration method, *Nucl. Technol.* 162 (2008), pp. 265-275.
- [2] K. Asakura, K. Takeuchi, T. Makino, Y. Kato, Feasibility study on a simplified MOX pellet fabrication process, the short process, for fast breeder reactor fuel, *Nucl. Technol.* 167 (2009), pp. 348-361.
- [3] R. L. Carr, Jr., Evaluating flow properties of solids, *Chem. Eng.* 18 (1965), pp. 163-168.
- [4] ASTM D6393-08, Standard Test Method for Bulk Solids Characterization by Carr Indices, ASTM International (2006)
- [5] T.Abe, T.Namekawa, K.Tanaka, "Oxide fuel fabrication technology development of the FaCT project (1) -overall review of fuel technology development of the FaCT project-" Proc.Global 2011, 513745, Dec. 11-16, 2011 Makuhari, Japan, (2011) [CD-ROM]
- [6] S.Takeda, "Predominant achievements of fuel cycle technology development in the FaCT project" Proc. Global 2011, 513284, Dec. 11-16, 2011 Makuhari messe, Japan, (2011), [CD-ROM]
- [7] H. Oshima, Development of microwave heating method for co-conversion of plutonium -uranium nitrate to MOX powder, *J. Nucl. Sci. Technol.* 26 (1989), pp. 161-166.
- [8] Y. Kato, T. Kurita, T. Abe, Dielectric properties of uranium and plutonium nitrate solution and the oxide compounds formed in the de-nitration process by the microwave heating method, *J. Nucl. Sci. Technol.* 41 (2004), pp. 857-862.
- [9] Y. Kato, T. Kurita, T. Abe, Reaction mechanism of de-nitration of $\text{UO}_2(\text{NO}_3)_2$ by the microwave heating[in Japanese], *Nihon-Genshiryoku-Gakkai Shi (J. At. Energy Soc. Jpn.)* 4[1] (2005), pp.77-83
- [10] M.Fuji, M.Takahashi, "Surface properties of particle and adhesion force between particles", Annual report of the ceramics research laboratory Nagoya institute of

technology, Vol.2, (2002), pp. 9-16.

- [11] S.M.Iveson, J.D.Litster, K.Hapgood, B.J.Ennis, "Nucleation, growth and breakage phenomena in agitated wet granulation process: a review" Powder technol. 117(2001) pp.3-39
- [12] K.Hotta, K.Takeda, K.Iinoya, "The capillary binding force of a liquid bridge" Powder tech., 10 (1974), pp. 231-242.

Figure captions

- Figure 1 Structure of the microwave heating apparatus
- Figure 2 A photograph of the microwave oven
- Figure 3 A photograph of the electric furnace
- Figure 4 Schematic diagrams and a photograph of the agitating granulator
- Figure 5 Typical SEM images showing particle distribution and fine structures of UO_2 and MOX raw powders
- Figure 6 Flow-ability and product yield of MOX granules in response to water addition ratio
- Figure 7 Typical particle size distributions of UO_2 and MOX raw powder
- Figure 8 Typical particle size distributions of UO_2 and MOX granules
- Figure 9 Typical SEM images showing particle distribution and fine structure of UO_2 and MOX granules
- Figure 10 Explanation of geometric parameters and dimensions of a liquid bridge between two equi-size spheres
- Figure 11 Typical photograph of MOX granules on a glass plate

Table 1 Specifications of examination apparatuses

Microwave de-nitration apparatus	<p>Microwave generators power: Max. 3.0 kW x 2</p> <p>Microwave frequency: 2455MHz ± 15MHz</p> <p>Capacity of microwave oven: 250 L</p> <p>Microwave tuner: E-H tuner</p> <p>De-nitration dish: Si₃N₄, 260 mm in dia. and 53 mm in depth</p>
Electric furnace for calcination and reduction	<p>Type: Rotary type</p> <p>Temperature range : R.T. - 1,000°C</p> <p>Heating rate: Max. 900°C/hr.</p> <p>Material: Inconel alloy</p>
Granulator	<p>Vessel effective capacity : 5 L</p> <p>Blade rotational speed : Agitator 110 - 1,000 rpm, Chopper 600 - 3,000 rpm</p> <p>Material: SUS 304</p>

Table 2 Specifications of analytical apparatuses

Distribution of particle diameter for raw powder	<p>Horiba, Ltd. Laser scattering particle size distribution analyzer Model LA-920</p> <p>Principle of measurement: Mie theory</p> <p>Measurement range: 0.02 - 2,000 μm</p>
Distribution of particle diameter for granules.	<p>Tokyo screen Co. Ltd. Test sieves (JIS Z8801)</p> <p>Material: Stainless steel, weave: Flat top weaving</p>
Flow-ability	<p>Hosokawa micron Co. Ltd. Powder tester Model PT-S</p>
Fine structure of a particle	<p>Hitachi, Ltd. Scanning Electron Microscope Model S-4300</p> <p>Type: Field emission, Resolution: 1.5nm, Magnification: 20 - 5 hundred thousand</p>
BET Specific surface area	<p>Shimadzu co. Ltd. Micromeritics FlowSorb II</p> <p>adsorption volume detection method: Continues flow,</p> <p>Measurement method: 1 point calibration methods</p>

Table 3 BET specific surface area and average particle size of raw powders

Sample	BET specific surface area (m ² /g)	Average particle size (μm)
U-1	1.5	1.0
U-2	1.6	1.1
U-3	2.0	1.5
MOX-1	2.4	1.4
MOX-2	2.6	1.2
MOX-3	2.4	1.8
MOX-4	2.5	1.8
MOX-5	2.8	1.6
MOX-6	3.3	1.3
MOX-7	2.4	1.5
MOX-8	2.4	1.5
MOX-9	2.3	1.4
MOX-10	2.9	1.6
MOX-11	2.6	1.5
MOX-12	3.8	1.3
MOX-13	2.4	1.4
MOX-14	2.5	1.5

Table 4 Characteristics and flow-abilities of raw powders

Sample	Bulk	Tap	Compressibility		Repose		Spatula		Aggregate		Flow-ability
	Density (g/cm ³)	Density (g/cm ³)	Ratio (%)	Point	Angle (°)	Point	Angle (°)	Point	Ratio (-)	Point	Index (-)
U-1	2.1	3.3	35	7	52	12	74	12	97	0	31
U-2	1.9	3.2	39	2	48	12	69	12	96	0	26
U-3	1.9	3.2	42	2	46	14.5	72	12	96	0	28.5
MOX-1	2.1	3.4	37	5	56	9.5	81	7	98	0	21.5
MOX-2	2.0	3.3	38	4.5	56	9.5	79	7	98	0	21
MOX-3	1.9	3.1	38	4.5	57	7	79	7	99	0	18.5
MOX-4	2.0	3.2	38	4.5	57	7	78	7	98	0	18.5
MOX-5	2.0	3.3	38	4.5	57	7	76	9.5	98	0	21
MOX-6	1.8	3.2	42	2	56	9.5	66	12	98	0	23.5
MOX-7	2.0	3.2	37	5	56	9.5	79	7	98	0	21.5
MOX-8	2.0	3.2	38	4.5	56	9.5	74	12	99	0	26
MOX-9	2.0	3.4	37	2	55	10	79	7	98	0	19
MOX-10	1.9	3.3	41	2	56	9.5	77	7	98	0	18.5
MOX-11	2.0	3.2	37	5	56	9.5	75	10	98	0	24.5
MOX-12	1.8	3.2	45	2	54	12	69	12	98	0	26
MOX-13	2.0	3.2	38	4.5	56	9.5	72	12	98	0	26
MOX-14	1.8	3.1	41	2	56	9.5	69	12	98	0	23.5

Table 5 BET specific surface area, average particle sizes and product yield of granules

Sample	Water addition ratio (wt. %)	BET specific surface area (m ² /g)	Average particle size (μm)	Product yield (%)
U-1	12	1.5	360	91
U-2	12.5	1.4	580	92
U-3	13	1.6	340	64
MOX-1	4	2.4	—	—
MOX-2	7	2.3	—	—
MOX-3	10	2.4	—	—
MOX-4	11	2.5	—	—
MOX-5	12.5	2.9	130	97
MOX-6	13	3.0	120	94
MOX-7	13	2.5	140	91
MOX-8	13	2.8	140	94
MOX-9	13.5	2.7	220	92
MOX-10	14	2.7	270	86
MOX-11	14	2.9	360	71
MOX-12	15	3.2	140	56
MOX-13	15	3.0	140	55
MOX-14	17	2.5	140	70

Table 6 Characteristics and flow-abilities of granules

Sample	Water addition ratio (wt %)	Bulk density (g/cm ³)	Tap density (g/cm ³)	Compressibility ratio		Repose angle		Spatula angle		Aggregate ratio		Flow-ability Index (-)
				(%)	Point	(°)	Point	(°)	Point	(-)	Point	
U-1	12	3.3	3.8	12	21	39	18	61	14.5	5	22.5	76
U-2	12.5	3.3	3.6	7	23	31	22	56	16	4	23	84
U-3	13	3.4	3.7	9	23	36	19.5	59	16	4	23	81.5
MOX-1	4	2.2	3.5	38	4.5	53	12	78	7	98	0	24
MOX-2	7	2.1	3.5	40	2	54	12	78	7	98	0	21
MOX-3	10	2.3	3.8	31	10	52	12	70	12	86	0	34
MOX-4	11	2.3	3.5	33	7	51	12	69	12	89	0	31
MOX-5	12.5	3.2	3.6	12	21	41	17	60	15	3	23	76
MOX-6	13	2.7	3.3	18	18	40	17.5	47	16	3	23	75
MOX-7	13	3.2	3.7	13	21	41	17	68	12	4	23	73
MOX-8	13	3.2	3.6	11	22	43	16	58	16	3	23	77
MOX-9	13.5	3.2	3.6	10	22.5	41	16	67	12	4	23	73.5
MOX-10	14	3.2	3.5	10	22.5	38	18	62	12	4	23	75.5
MOX-11	14	3.2	3.5	10	22.5	36	19.5	47	16	5	22.5	80.5
MOX-12	15	2.6	3.4	24	16	38	18	49	16	3	23	73
MOX-13	15	3.4	3.7	10	22.5	42	16	58	16	3	23	77.5
MOX-14	17	3.4	3.9	13	21	43	16	55	16	4	23	76

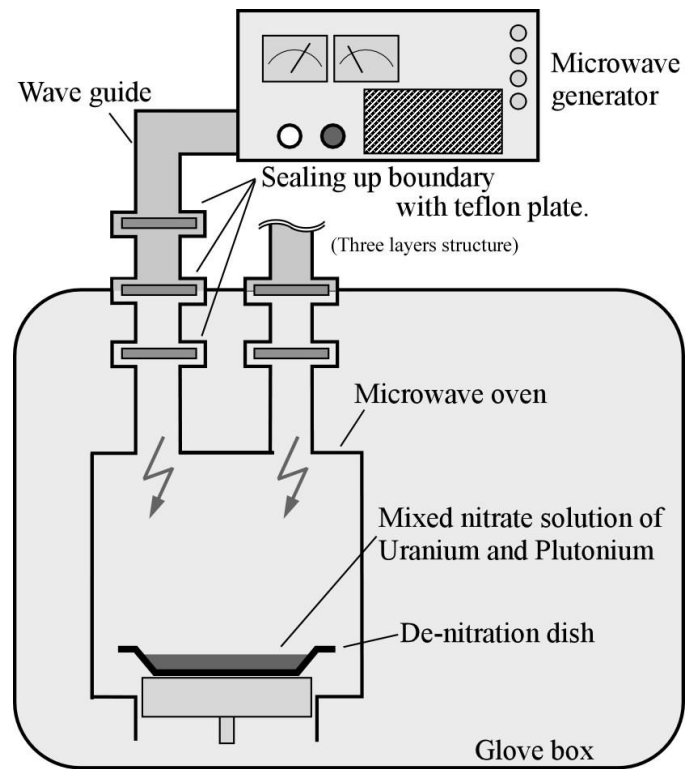


Figure 1 Structure of the microwave heating apparatus



Figure 2 A photograph of the microwave oven

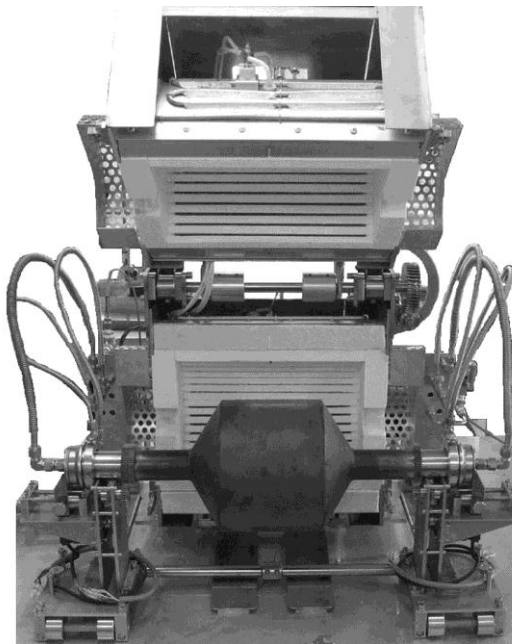
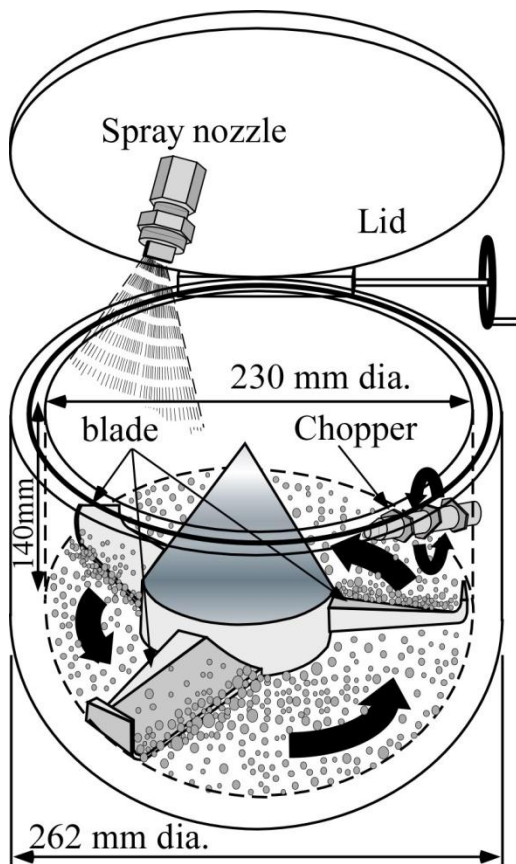
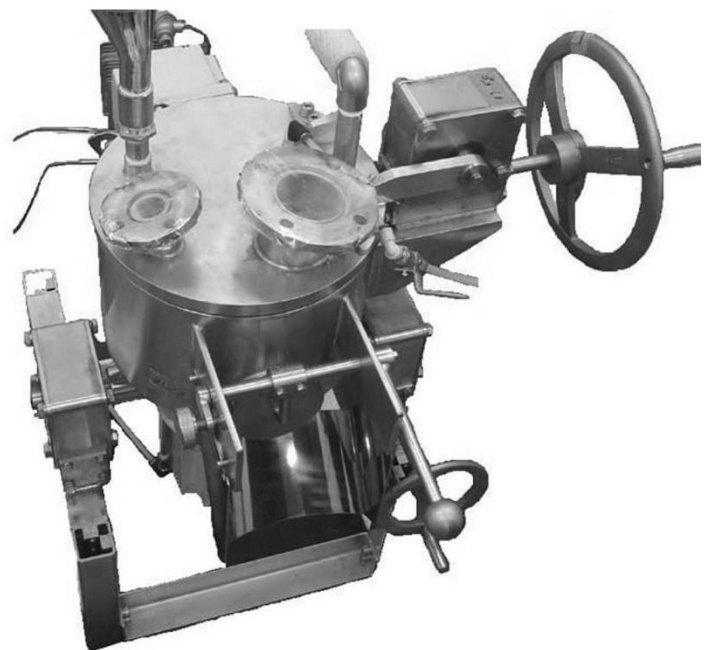


Figure 3 A photograph of the electric furnace

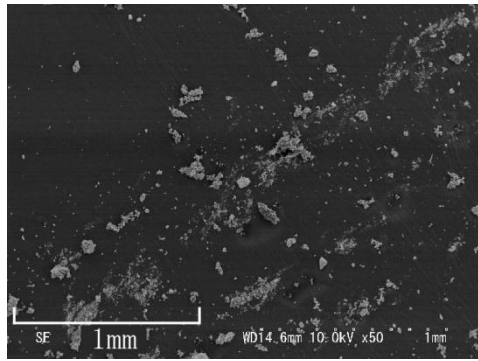


(a)

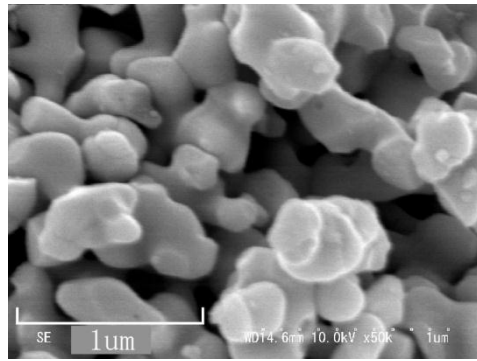


(b)

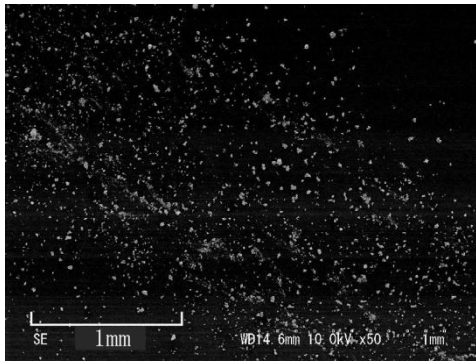
Figure 4 Schematic diagrams and a photograph of the agitating granulator



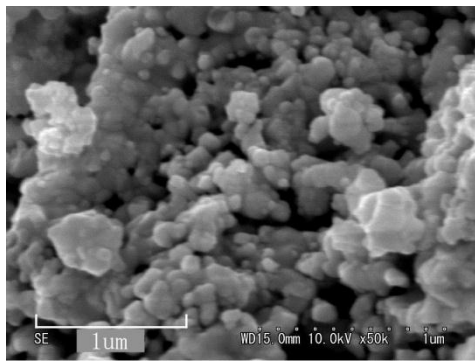
(a) Sample U-1 (Low magnification)



(b) Sample U-1 (High magnification)



(c) Sample MOX-7 (Low magnification)



(d) Sample MOX-7 (High magnification)

Figure 5 Typical SEM images showing particle distribution and fine structure of UO_2 and MOX raw powders.

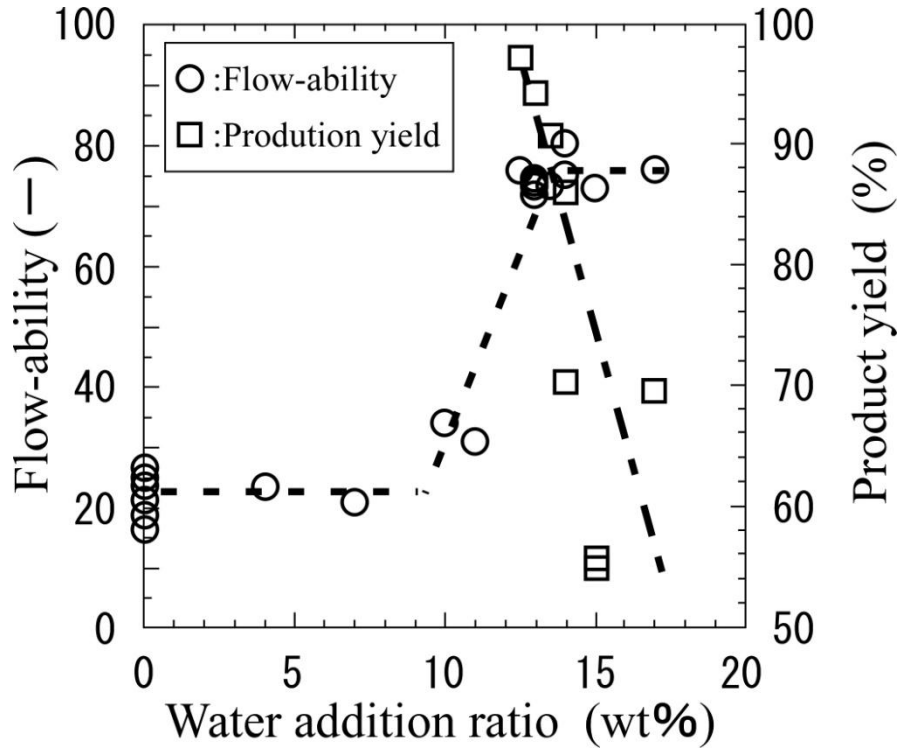
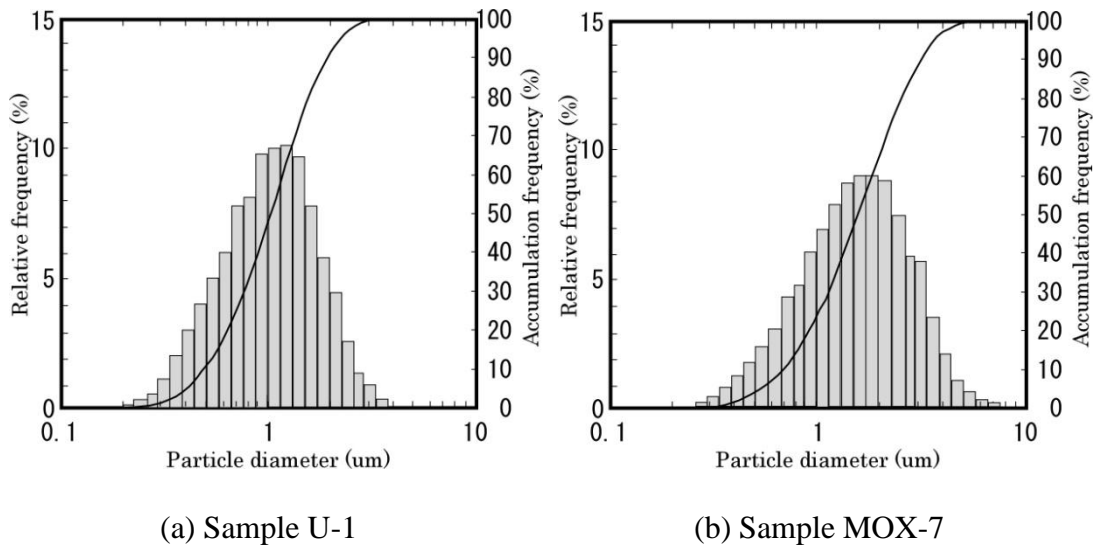


Figure 6 Flow-ability and product yield of MOX granules in response to water addition ratio



(a) Sample U-1 (b) Sample MOX-7

Figure 7 Typical particle size distributions of UO_2 and MOX raw powders

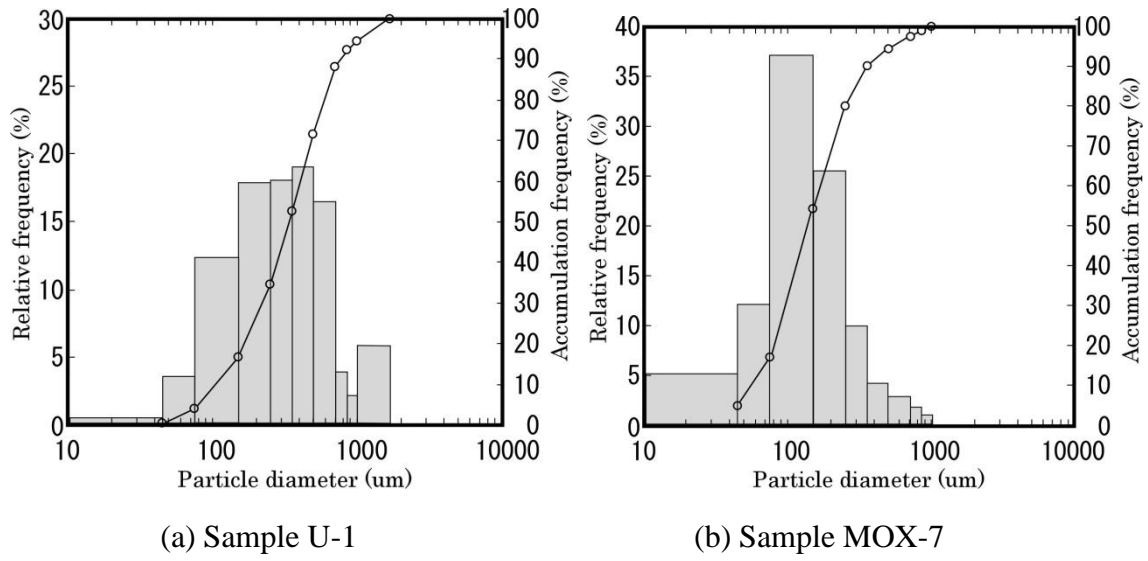
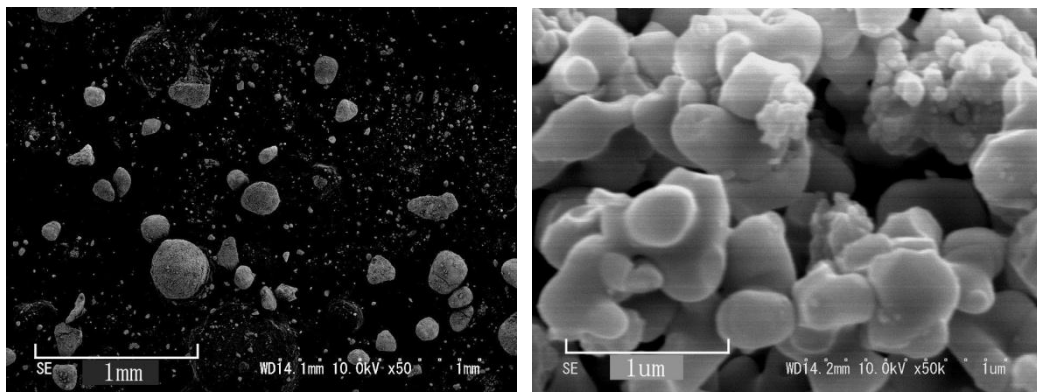
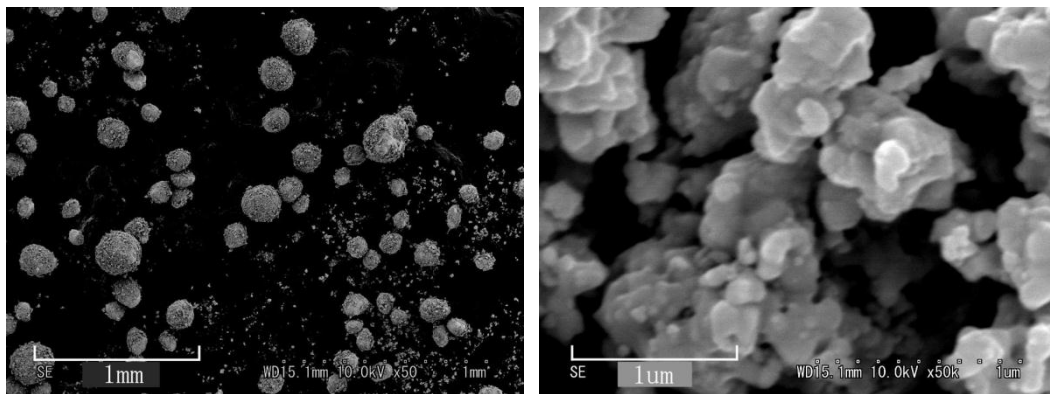


Figure 8 Typical particle size distributions of UO_2 and MOX granules



(a) Sample U-1 (Low magnification) (b) Sample U-1 (High magnification)



(c) Sample MOX-7 (Low magnification) (d) Sample MOX-7 (High magnification)

Figure 9 Typical SEM images showing particle distribution and fine structures of UO_2 and MOX granules

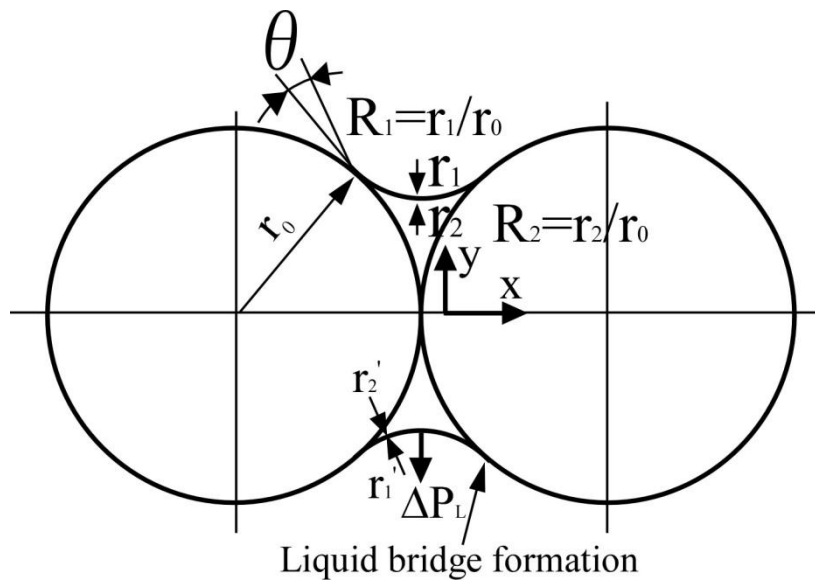


Figure 10 Explanation of geometric parameters and dimensions of a liquid bridge between two equi-size spheres.

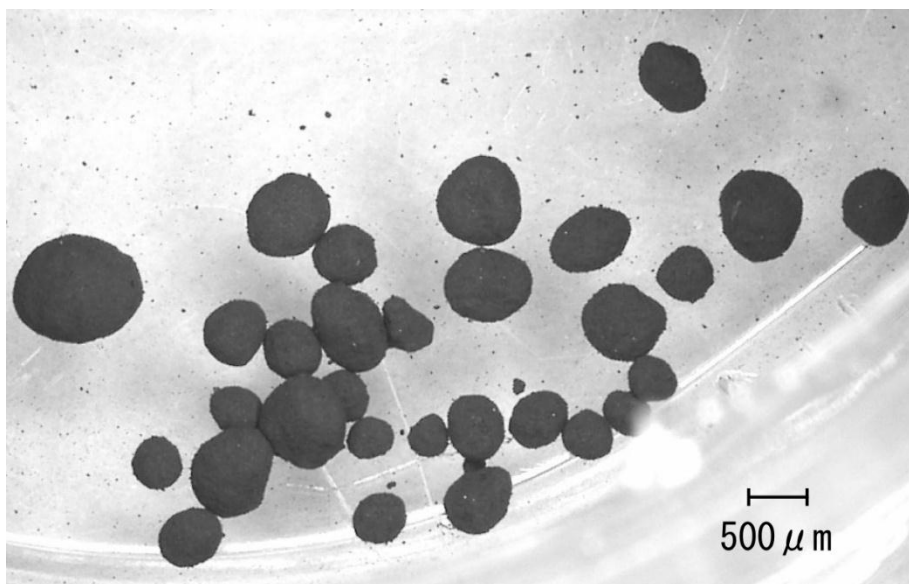


Figure 11 Typical photograph of MOX granules on a glass plate.